

PCCP

Accepted Manuscript



This is an *Accepted Manuscript*, which has been through the Royal Society of Chemistry peer review process and has been accepted for publication.

Accepted Manuscripts are published online shortly after acceptance, before technical editing, formatting and proof reading. Using this free service, authors can make their results available to the community, in citable form, before we publish the edited article. We will replace this *Accepted Manuscript* with the edited and formatted *Advance Article* as soon as it is available.

You can find more information about *Accepted Manuscripts* in the [Information for Authors](#).

Please note that technical editing may introduce minor changes to the text and/or graphics, which may alter content. The journal's standard [Terms & Conditions](#) and the [Ethical guidelines](#) still apply. In no event shall the Royal Society of Chemistry be held responsible for any errors or omissions in this *Accepted Manuscript* or any consequences arising from the use of any information it contains.



Journal Name

ARTICLE

Phase Transitions in Hydrophobe/Phospholipid Mixtures: Hints at Connections between Pheromone and Anaesthetic Action

Received 00th January 20xx,
Accepted 00th January 20xx

Silvia Borsacchi,^a Marco Geppi,^b Sara Macchi,^b Barry W. Ninham,^c Emiliano Fratini,^d Moira Ambrosi,^d Piero Baglioni^{d,e} and Pierandrea Lo Nostro^{*d,e}

DOI: 10.1039/x0xx00000x

www.rsc.org/

The phase behavior of mixtures of a typical insect pheromone (olean) and a phospholipid (DOPC)/water dispersion is extensively explored through SAXS, NMR and DSC experiments. The results mimic those obtained with anaesthetics in phospholipid/water systems. They also mimic the behavior and microstructure of ternary mixtures of membrane mimetic, bilayer-forming double chained surfactants, oils and water. Taken together with recent models for conduction of the nervous impulse, all hint at lipid involvement and an underlying unity in mechanisms of pheromone, anaesthetic and hydrophobic drugs, where a local phase change in the lipid membrane architecture may be at least partly involved in the transmission of the signal.

1. Introduction

Light detection with fireflies, chemical pheromones, general and local anaesthetics, cationic surfactants as immunosuppressants, cationic polymers as poisons and muscle relaxants, and other drugs, all involve interactions with the membrane of the nerve axon. The phase changes induced in the lipid membrane are all reversible. At least partly, the mechanisms must be physical, not only biochemical.¹

The implications are that induced microstructure provides a unified mechanism that interplays with several biophysical processes such as nerve conduction, anaesthetics and pheromone activities.

The outline of this paper is as follows:

We briefly recall in the Introduction the implication of phase changes in anaesthetics and pheromone activity and we shortly present the experimental approach of this work. We then report our results on the uptake of a highly hydrophobic molecule into a biomimetic lipid bilayer and the resulting phase changes that occur. At the end, we discuss the

experimental results in the light of a combined mechanism, that at least partly involves physical chemistry and not only biochemistry.

1.1 Anaesthetics

If the lipid phase transition model captures some essentials of mechanism, and specifically, involves a cubic-lamellar phase transition, then the action of anaesthetics may be at least partly attributed to changes in membrane structure induced by adsorption of a hydrophobe.

The mechanism by which general anaesthetics operate is still unknown and controversial.^{2,3}

Neither the Meyer-Overton rule (or lipid theory), nor the protein theory can explain satisfactorily all the experimental evidence.³ The former is based on the general hydrophobic nature of anaesthetics, that results in their great solubility in the hydrocarbon chain pocket. The latter is based on the evidence that anaesthetics bind specifically with proteins such as serum albumin and adenylate kinase, and activate receptors or ion channels. The interaction of different local and general anaesthetics with vesicles⁴⁻⁶ and planar bilayers^{7,8} supported on solid substrates has been approached in previous contributions. The interested reader can refer to some relevant reviews on the subject.⁹⁻¹² Here we just recall that (i) the effect of anaesthetics seems to be related to the hydration of biomembranes,^{13,14} (ii) effective anaesthetics (*e.g.* CHCl₃) need to be at least slightly polar to reside close to the interface of the bilayer,^{3,13,15-32} (iii) the active molecule directly interacts with the membrane lipids, and thus modifies the fluidity, the curvature and phase structure of the bilayer which in turn alters the conformation and functional performances of ion channels, receptors and more in general of transmembrane

^a Istituto di Chimica dei Composti Organometallici (ICCOM) del CNR, 56124 Pisa, Italy

^b Department of Chemistry and Industrial Chemistry, University of Pisa, 56124 Pisa, Italy

^c Department of Applied Mathematics, Research School of Physical Sciences and Engineering, Australian National University, Canberra, ACT 0200, Australia.

^d Department of Chemistry & CSGI, University of Florence, 50019 Sesto Fiorentino (Firenze), Italy.

^e Enzo Ferroni Foundation, 50019 Sesto Fiorentino (Firenze), Italy.

* Corresponding author. Email: PLN@csgi.unifi.it; Tel: +39 055 457-3010; Fax: +39 055 457-3036.

† Electronic Supplementary Information (ESI) available: [details of any supplementary information available should be included here]. See DOI: 10.1039/x0xx00000x

proteins,^{3,16-22} (iv) finally according to a more recent view, certain membrane proteins are clustered in cholesterol-rich “lipid rafts”, *i.e.* transient micro-phase separated domains in a liquid ordered phase (L_o), with characteristics intermediate between those of a gel and of a liquid-crystalline phase, in coexistence with a fluid-like liquid disordered phase (L_d).^{23,24} In passing we recall that the effect of small hydrophobic chemicals such as chloroform or diethyl ether on phospholipid model membranes has been the object of a great number of works as for example in Refs. 22 and 26.

Probably the origin of the anaesthetic action is manifold and there is no single switch to induce anesthesia. As clinical experiments suggest, multiple neurotransmission factors respond to anesthetics with high cooperativeness, and presumably the lipid rearrangement is one of them.²⁸

1.2 Pheromones

Pheromones are molecules that are produced by one individual and act as ectohormones to hijack behavior when detected by another member of the same species.³³ Several pheromones, particularly those produced by insects, are lipid molecules such as ketones, aldehydes and fatty acids,³⁴ more or less volatile.³⁵ Usually volatile pheromones are detected by olfactory receptors, while low- or non-volatile pheromones are detected via contact chemosensory receptors distributed across the body.³⁵ In particular queen pheromones, that signal the presence of a fertile queen and induce daughter workers to remain sterile as in bees, termites, ants, etc., contain both volatile and non-volatile components.³⁶ The way pheromones work is the object of several studies. Recently it was found that free fatty acids act as ligands for gypsy moth's pheromone and control their adsorption on hydrophobic surfaces.³⁷

The work in this paper explores the phase behavior of hydrophobic pheromone/phospholipid mixtures in water dispersions. We note that there is no difference in the chemistry of pheromone or anaesthetic molecules. We deduce that there is nothing magic with either in their influence in modifying the lipid membrane nanostructure. That observation sits well with the known fact that pheromones in excess do behave as anaesthetics.³⁸

With these premises we decided to explore membrane changes induced by an anaesthetic-like pheromone. The molecule chosen was 1,7-dioxaspiro[5.5]undecane or “olean” (Figure 1), the major component of the sex pheromone of the olive fly (*Bactrocera oleae* Gmelin). According to some preliminary tests, olean is a potent killer for other insect species (*e.g.* mosquitoes) at relatively high concentration (data to be published). In any event, we have reasonable expectations that any pheromone induced phase behavior may well mimic that of anaesthetic molecules and provide hints at mechanism for both.

1.3 Experimental approach

In order to investigate in detail the phase changes induced in a biomimetic lipid bilayer by the presence of a pheromone, we performed small angle X-ray scattering (SAXS), differential

scanning calorimetry (DSC) and multinuclear magnetic resonance spectroscopy (NMR) experiments on a series of samples containing an aqueous dispersion of dioleoylphosphatidylcholine (DOPC), and increasing amounts of olean. Moreover, dispersions of DOPC in deuterated water, with different concentrations of olean, were prepared and studied through ^2H -NMR. In addition, aqueous dispersions of DOPC containing deuterated cyclohexane (d_{12}) were prepared and investigated. Since the deuterated form of olean is not commercially available, and because of its cyclic structure and similar polarity, cyclohexane was chosen to mimic the pheromone molecule.

2. Experimental section

2.1 Chemicals

1,7-dioxaspiro[5.5]undecane or “olean” (Figure 1), was purchased from Alfa Aesar (Heysham, United Kingdom; purity > 98%) and used without further purification.

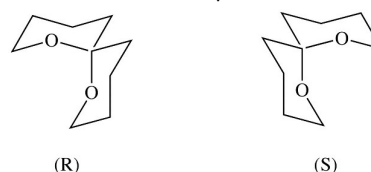


Figure 1. Chemical structure of 1,7-dioxaspiro[5.5] undecane (“olean”).

Dioleoylphosphatidylcholine (DOPC) was supplied by Avanti Polar Lipids (Birmingham, Alabama) and used without further purification. Cyclohexane- d_{12} and deuterium oxide were supplied by Sigma-Aldrich (Milan, Italy) and used as received.

Samples Preparation

A 60% w/w stock dispersion of DOPC/ H_2O and of DOPC/ D_2O (mole ratio 1:30) was prepared. At this concentration and at 25° C the system forms a lamellar phase.³⁹ The samples were annealed through repeated heating-cooling cycles, then centrifuged and stirred. The same treatment was applied to the samples containing the hydrophobe, either the pheromone or cyclohexane- d_{12} , with a hydrophobe/DOPC mole ratio ranging between 0:1 and 10:1. All the samples were left to equilibrate for a week in a refrigerator before performing the experiments. All samples at all concentrations were – at least macroscopically - homogeneous. No phase separation was ever detected after the sample preparation.

2.2 NMR

^{31}P , ^2H , ^{13}C and ^1H -NMR spectra were acquired on a Varian Infinity Plus 400 spectrometer, working at a Larmor frequency of 161.94, 61.41, 100.58 and 400.03 MHz for ^{31}P , ^2H , ^{13}C and ^1H , respectively, equipped with a 5-mm goniometric probe.

The 90° pulse duration for ^{31}P , ^2H , ^{13}C and ^1H was 3.0, 3.5, 4.0 and 4.4 μs , respectively. All the spectra were acquired in static conditions. ^{31}P spectra were acquired with ^{31}P direct excitation with high power decoupling from ^1H , with a recycle delay of 5 s, and accumulating 2048 transients. ^2H spectra were acquired with the quadrupolar echo pulse sequence (90°_x – τ – 90°_y – τ – acquisition), with a τ of 20 μs , a recycle delay of 2.5 s, and

accumulating 32768 transients. ^{13}C direct excitation spectra were acquired using a DEPTH pulse sequence for eliminating the probe background signal,⁴⁰ with high-power decoupling from protons, using a recycle delay of 3 s, and accumulating 4096 transients. ^1H T_1 were measured with the saturation recovery sequence, with delays varying from 0.01 to 30 s. ^2H T_1 were measured with the inversion recovery sequence with delays varying from 0.1 to 2 s. ^{31}P spectral simulations were performed using the WSOLIDS software developed in the group of Roderick Wasylshen.⁴¹ ^{31}P , ^2H and ^{13}C chemical shifts were referred to phosphoric acid (85 wt%, 0 ppm), D_2O (0 ppm) and dodecane as secondary reference, respectively, and they were referred to TMS as primary reference. All experiments were carried out at 25 °C.

2.3 SAXS

Small angle X-Ray scattering (SAXS) measurements were carried out with an HECUS SWAX-camera (Kratky) equipped with a position-sensitive detector (OED 50M) containing 1024 channels of width 54 μm . $\text{Cu K}\alpha$ radiation of wavelength, $\lambda = 1.542 \text{ \AA}$, was provided by a Seifert ID-3003 X-ray generator (sealed-tube type), operating at a maximum power of 2 kW. A 10 μm thick nickel filter was used to remove the $\text{Cu K}\beta$ radiation. The sample-to-detector distance was 273 mm. The volume between the sample and the detector was kept under vacuum during the measurements to minimize scattering from the air. The Kratky camera was calibrated in the small angle region using silver behenate ($d = 58.38 \text{ \AA}$).⁴² Scattering curves were obtained in the Q-range between 0.01 and 0.54 \AA^{-1} , Q being the scattering vector $4\pi(\sin\theta)/\lambda$, and 2θ the scattering angle. Paste-like samples were filled into a 1 mm demountable cell having kapton-film as windows. The temperature was controlled by a Peltier element, with an accuracy of $\pm 0.1 \text{ }^\circ\text{C}$. All scattering curves were corrected for the empty cell contribution considering the relative transmission factor. SAXS curves were iteratively desmeared using the procedure reported by Lake.⁴³

2.4 DSC

Differential scanning calorimetry (DSC) runs were performed with a Q1000 (TA Instruments) apparatus using aluminum hermetic pans. For each phase transition the peak temperature and the corresponding enthalpy change (ΔH) were evaluated. The samples were purged with N_2 (50 mL min^{-1}). The temperature investigated ranged between $-60 \text{ }^\circ\text{C}$ and $40 \text{ }^\circ\text{C}$, at a heating rate of $2 \text{ }^\circ\text{C min}^{-1}$. A slower scan rate did not modify the thermogram profile.

3. Results and discussion

3.1 SAXS

SAXS measurements (Figure 2) confirm that a 60% w/w dispersion of DOPC in water, our biomimetic lipid bilayer, consists in a lamellar phase (L_α) with a spacing $d = 51.50 \text{ \AA}$.³⁹ When the pheromone is uploaded to a 1:1 mole ratio the SAXS pattern still indicates the presence of a lamellar phase, but

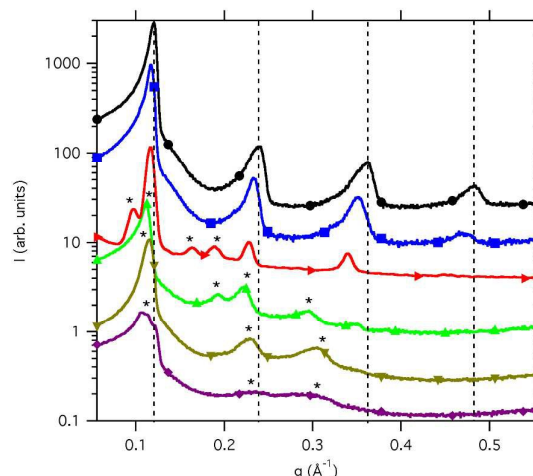


Figure 2. SAXS profiles of a pure 60% w/w DOPC aqueous dispersion (●), and at different pheromone/DOPC mole ratios: 1:1 (■), 2:1 (▴), 4:1 (▲), 6:1 (▼), and 10:1 (◆). The asterisks denote the peaks due to the inverse hexagonal phase.

with an increment in the d spacing up to 53.07 \AA (squares in Figure 2).

Figure 3 shows the SAXS profile for a pheromone/DOPC mole ratio of 2:1, suggesting the coexistence of lamellar (L_α) and inverse hexagonal (H_{II}) phases. This result will be confirmed by ^{31}P NMR experiments (see below).

For a pheromone/DOPC mole ratio of 4:1 the SAXS profile indicates the presence of an inverse hexagonal phase with a spacing of 64.10 \AA (up-pointing triangles in Figure 2)

A further increment in the pheromone concentration induces a reduction in the extension of the ordered domain and in the d spacing, down to 62.12 \AA for a mole ratio of 6:1 and 60.46 \AA for a mole ratio of 10:1. The broadening of the peaks reflects a significant loss in the long range structure.

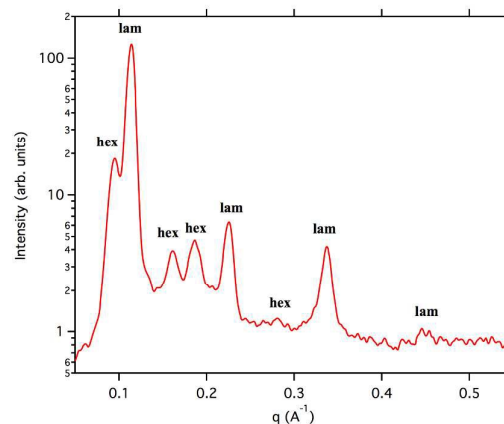


Figure 3. SAXS profile for 60 % w/w DOPC aqueous dispersion containing a 2:1 pheromone/DOPC mole ratio. The peaks typical of a lamellar (lam) and of an inverse hexagonal (hex) phase are indicated.

Table 1 summarizes the DOPC/water phases observed for the different pheromone/DOPC mole ratios (c) and the corresponding spacings (d) obtained from SAXS measurements.

Table 1. d spacings (in Å) and phase description for the investigated DOPC/water/pheromone samples at different pheromone/DOPC mole ratios (c).

c	d (Å)	phase
0:1	51.5	L_{α}
1:1	53.1	L_{α}
2:1	55.3	L_{α}
2:1	66.5	H_{II}
4:1	64.1	H_{II}
6:1	62.1	H_{II}
10:1	60.5	H_{II}

Figure 4 and 5 show the structure of a L_{α} and of a H_{II} phase, respectively, and the structural parameters that can be calculated from the experimental spacings d , indicated as d_{lam} and d_{hex} for the L_{α} and H_{II} phase, respectively, according to equations 1-9.⁴⁴

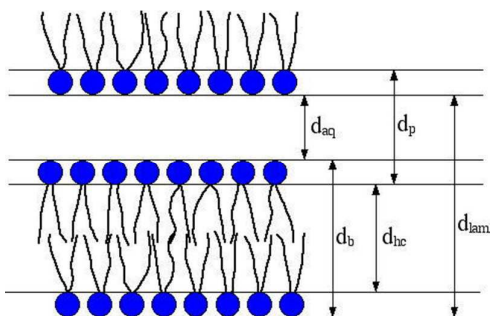


Figure 4. Structure of a lamellar (L_{α}) phase. d_{lam} is the experimental spacing directly obtained from SAXS measurements (see Table 2). d_{hc} is twice the length of the hydrocarbon chains, d_b is twice the length of the entire phospholipid, d_{aq} is the thickness of the water pool, and d_p is the thickness of the polar region (including the two facing layers of polar heads). A_p is the polar head cross section. d_{hc} , d_b , d_{aq} , d_p and A_p can be obtained from d_{lam} through equation 1-5. Adapted with permission.⁴⁴ Copyright 1994, Elsevier Ltd.

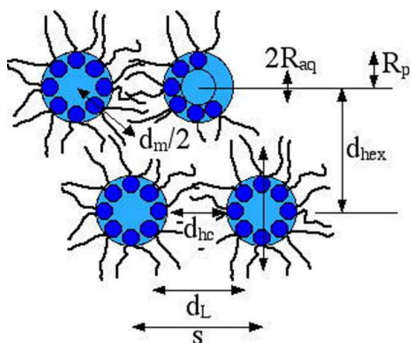


Figure 5. Structure of an inverse hexagonal phase (H_{II}). d_{hex} is the experimental spacing directly obtained from SAXS measurements (see Table 3). R_{aq} is the radius of the water inner pool, R_p is the radius of the hydrophilic compartment, including the thickness of the polar head, d_m is the distance between the centers of two diagonal cylinders, s is the center-to-center distance between two adjacent cylinders, and d_L is given by d_{hc} and twice the thickness of the polar head. R_{aq} , R_p , d_m , s and d_L can be obtained from d_{hex} through equation 6-9. Adapted with permission.⁴⁴ Copyright 1994, Elsevier Ltd.

$$d_b = \frac{v_l + cv_{phe}}{v_{aq} + v_l + cv_{phe}} d_{lam} = \phi d_{lam} \quad (1)$$

$$A_p = \frac{2(v_l + cv_{phe})}{d_b} \quad (2)$$

$$d_{hc} = \frac{2(v_{hc} + cv_{phe})}{A_p} \quad (3)$$

$$d_{aq} = d_{lam} - d_b \quad (4)$$

$$d_p = \frac{2(v_{aq} + v_p)}{A_p} \quad (5)$$

$$s = \frac{2d_{hex}}{\sqrt{3}} \quad (6)$$

$$R_{aq} = \sqrt{\frac{2d_{hex}^2(1-\phi)}{\pi\sqrt{3}}} \quad (7)$$

$$d_L = s - 2R_{aq} \quad (8)$$

$$d_m = 2\left(\frac{s}{\sqrt{3}} - R_{aq}\right) \quad (9)$$

v_l is the volume of one phospholipid molecule, ϕ is the volume fraction of the phospholipid and the pheromone, v_{aq} is the volume of water per phospholipid molecule, v_{hc} is the volume of the hydrocarbon chains, v_{phe} is the volume of the pheromone, c is the pheromone/DOPC mole ratio and v_p the volume of the polar part.⁴⁴ Since the pheromone molecules are completely soluble in an apolar solvent such as *n*-decane, we assume that they are located in the hydrophobic portion of the bilayer and of the inverse hexagonal phase. Moreover, since the olefin molecule is hindered and stiff, we assume that once in the lamellar or in the inverse hexagonal phase, it will retain its molecular volume as in the pure liquid state. For the calculations, the molecular volume of water is taken as 30 \AA^3 at $20 \text{ }^\circ\text{C}$ and the number of hydration molecules around the DOPC polar heads is 9.³⁹ The volume of a single DOPC molecule (v_l) is 1290 \AA^3 , the volume occupied by the polar head (v_p) is 374 \AA^3 , while that occupied by the hydrophobic chains (v_{hc}) is 916 \AA^3 .^{44,45} The volume of a pheromone molecule in the liquid state (v_{phe}) was calculated from its density and is 254 \AA^3 . Table 2 and 3 list the structural parameters and the volume fractions for the samples investigated.

The data obtained for pure DOPC/water agree with those reported in the literature.^{39,46}

The uptake of the pheromone molecules brings about an increment of 4 \AA in d_{hc} spacing as a consequence of the thicker hydrophobic portion of the lipid bilayer in the lamellar phase. In fact d_b and d_{hc} increase, while d_{aq} and d_p decrease.

Table 2. Structural parameters for the lamellar phase (see Figure 4) at two different pheromone/DOPC mole ratios (c) calculated according to equations 1-5.

c	ϕ	d_{lam} (Å)	d_b (Å)	A_p (Å ²)	d_{aq} (Å)	d_p (Å)	d_{hc} (Å)
0:1	0.8269	51.5	42.6	60.6	8.9	21.3	30.2
1:1	0.8512	53.1	45.2	68.4	7.9	18.8	34.2

Table 3. Structural parameters for the inverse hexagonal phase (see Figure 5) at different pheromone/DOPC mole ratios (c) calculated according to equations 6-9.

c	ϕ	d_{hex} (Å)	s (Å)	R_{aq} (Å)	d_L (Å)	d_m (Å)
4:1	0.8952	64.1	74.0	12.6	48.8	60.3
6:1	0.9125	62.1	71.7	11.1	49.5	60.6
10:1	0.9341	60.5	69.9	9.4	51.1	61.9

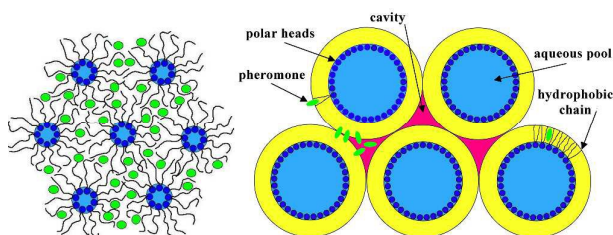


Figure 6. Inverse hexagonal array in the aqueous dispersion of DOPC after the uptake of the pheromone molecules (in green). The dark blue spots represent the polar heads of the phospholipid, while the light blue regions indicate the inner water pool, the yellow layers are the hydrophobic portion of the nanostructure, and the red area is the inter-cylinder region occupied by the pheromone molecules.

In the case of the inverse hexagonal phase (Figures 5 and 6) the further addition of pheromone to the sample with a pheromone/DOPC mole ratio (c) of 4:1 reduces the thickness d_{hex} and the distance between the centres, s , of the cylinders of about 4 Å (see Table 3).

This change produces a more compact structure, with a reduction of the water pool size from 12.6 to 9.4 Å. On the other hand, the distance d_m increases from 60.3 to 61.8 Å. These results suggest that the pheromone molecules occupy the cavity between the cylinders, as shown in , with a significant stabilization of the structure.⁴⁷

For c greater than 10:1 the amount of pheromone is so large that it cannot be dispersed into the cavities, and the sample loses its long range structure, as suggested by the broad peak in the SAXS pattern (diamonds in Figure 2).

3.2 DSC

The thermograms of the investigated DOPC/water/pheromone samples show the presence of two peaks during the cooling and two peaks during the heating scan. In order to avoid problems related to overcooling effects, we have considered only the heating peaks (see Figure S1 in the ESI†).

In the case of a 60% aqueous dispersion of DOPC the liquid crystal-lamellar phase transition (L_c - L_α) is found at -16.8 °C, with a corresponding enthalpy change of about $35.0 \text{ kJ mol}^{-1}_{\text{DOPC}}$ (Figure 7). These values agree with those reported in the literature for a water/DOPC mole ratio of 30.^{39,48} The melting of water in the pure DOPC aqueous dispersion occurs at -0.2 °C (Figure 7).

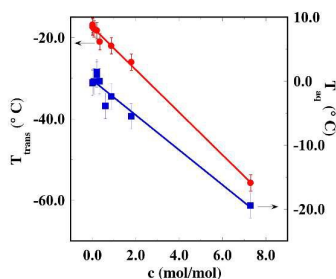


Figure 7. L_c - L_α phase transition temperature (T_{trans} , red line), and water melting temperature (T_{aq} , blue line) as a function of the pheromone/DOPC mole ratio (c). The error bars represent the standard deviation.

As reported by Ulrich the sub-zero melting of the phospholipid's acyl chains occurs in the presence of frozen ice, instead of liquid water.³⁹ This is the reason why the thermal behavior of unsaturated lipids differs from that of saturated lipids. In turn, when ice melts around 0° C the unsaturated hydrophobic tails are in a liquid state (L_α phase). This occurrence, together with the thermally induced fluctuations and undulations in the bilayer brings about an increment in the head group cross section that results in a lowering of the chemical potential of the hydrating water molecules that reside near the bilayer interface.^{26,49-51} Hence, the water melting point decreases and the polar heads undergo relatively small conformational adjustment.^{39,52} Furthermore, the addition of the hydrophobic pheromone to the DOPC dispersion increases the disorder in the hydrophobic layer and therefore the $L_c \rightarrow L_\alpha$ phase transition temperature decreases. Further additions of pheromone induce the formation of the H_{II} phase and lower the $L_\alpha \rightarrow H_{II}$ transition temperature.⁵³ The water melting temperature remains almost constant (see the blue line in Figure 7) up to the 1:1 pheromone/DOPC mole ratio, and then decreases down to -19.4 °C. We recall that water pore-confined into the rod-like micelles of the H_{II} phase freezes below 0 °C.⁵⁴ The enthalpy change (ΔH_{trans}) associated to the L_c - L_α transition does not vary significantly until a pheromone/DOPC mole ratio of 8:1 is reached, where a cubic phase is formed, as indicated by the NMR measurements (see below).

3.3 NMR

NMR experiments were performed on DOPC/ D_2O /pheromone and DOPC/ H_2O /cyclohexane- d_{12} samples, as a function of the pheromone and of the deuterated cyclohexane concentration.

3.3.1 ^{31}P NMR

^{31}P static spectra allow a straightforward determination of the chemical shift tensor of ^{31}P nuclei, that are particularly effective in identifying the phases formed in phospholipid/water dispersions.^{55,56}

The spectra recorded for the pure DOPC/ D_2O dispersion and after the uptake of different amounts of pheromone are reported in Figure 8 along with the corresponding spectral simulations: the spectral parameters obtained from the simulations are reported in Table 4.

The lineshape of the spectrum for the DOPC/ D_2O system clearly indicates the presence of a single L_α phase,^{55,56} confirming the SAXS results. By adding increasing amounts of pheromone the ^{31}P spectrum remains substantially unchanged up to a pheromone/DOPC mole ratio 0.5:1. For the 1:1 ratio a very small amount of a second phase is revealed by the small signal at about 10 ppm. This signal becomes more evident at higher pheromone amounts. The spectral parameters obtained by simulation clearly indicate that this second phase is an inverse hexagonal phase H_{II} . At much higher pheromone contents (5:1 ratio) the H_{II} phase coexists with an isotropic inverse cubic I_{Hc} phase, which gives rise to the narrow isotropic signal superimposed to that of the H_{II} phase. The same

experiments were performed on the DOPC/H₂O/cyclohexane-d₁₂ system. DOPC/H₂O gave exactly the same spectrum as DOPC/D₂O.

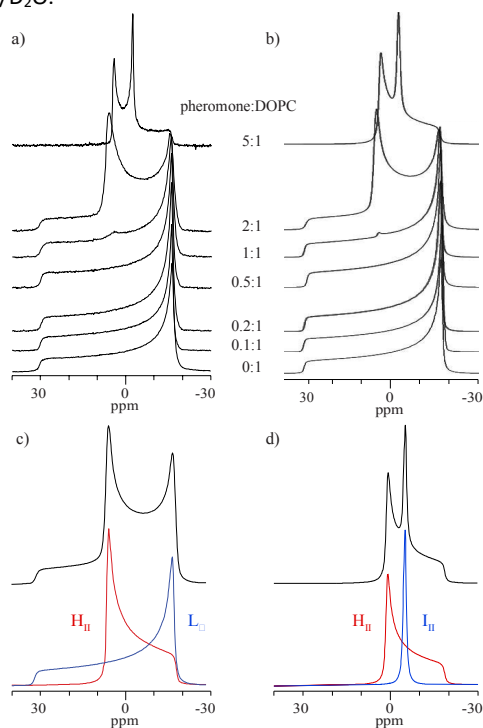


Figure 8. Upper part: experimental (left) and simulated (right) ³¹P NMR spectra of 60% w/w DOPC/D₂O dispersion with different concentrations of pheromone. Lower part: simulated ³¹P NMR spectra of two DOPC/D₂O/pheromone samples highlighting the spectral contributions of L_{II}, H_{II} and I_{II} phases.

The uptake of cyclohexane-d₁₂ had a very similar effect on the phase behavior of the whole system, with the onset of an L_α-H_{II} transition for the sample with a 1:1 mole ratio (2% of H_{II}, regularly increasing at higher cyclohexane amounts), in perfect agreement with the results obtained for the DOPC/D₂O/pheromone samples (spectra not shown). The only difference between the two sets of samples is that no isotropic I_{II} phase formed even at an 8:1 pheromone/DOPC mole ratio appears. The strong likeness of the phase behavior of these two sets of samples further supports the choice of cyclohexane as a deuterated hydrophobic model molecule for mimicking the effects produced by the pheromone.

Table 4. Phase formed, its percentage and chemical shift tensor δ parameters of the corresponding DOPC ³¹P sites in 60% w/w DOPC/D₂O dispersions containing different amounts of pheromone, as obtained from simulations of the experimental ³¹P NMR spectra. The chemical shift parameters are indicated according to the Herzfeld-Berger convention:⁵⁷ $\delta_{11} \geq \delta_{22} \geq \delta_{33}$ (in ppm) are the principal values of the δ tensor, Ω (ppm) = $\delta_{11} - \delta_{33}$, δ_{iso} (ppm) = $(\delta_{11} + \delta_{22} + \delta_{33})/3$, $k = 3(\delta_{22} - \delta_{iso})/\Omega$. The uncertainties on the values of percentages, δ_{iso} and Ω are ± 1 , ± 0.1 and ± 0.1 , respectively.

c	phase	% of phase	Ω (ppm)	δ_{iso} (ppm)	k
0:1	L _α	100	46.8	0.1	-1
0.1:1	L _α	100	46.5	0.2	-1
0.2:1	L _α	100	46.2	0.1	-1
0.5:1	L _α	100	46.5	0.2	-1
1:1	L _α	98	46.4	0.2	-1
	H _{II}	2	21±2	-11±1	1
2:1	L _α	53	46.8	0.3	-1
	H _{II}	47	23.1	-0.2	1
5:1	H _{II}	79	20.9	-1.4	1
	I _{II}	21	-	-1.3	-

3.3.2 ¹³C NMR

¹³C static spectra were recorded in order to study the structural and dynamic properties of the phospholipid chains. The spectra of DOPC/D₂O/pheromone samples, reported in Figure 9, show a very good resolution. They were recorded under static conditions, which means that the residual chemical shift anisotropy (CSA) of the ¹³C nuclei is very small and that, therefore, both the pheromone and the phospholipid chains are in quite mobile environments.

1,2-dioleoyl-*sn*-glycero-3-phosphatidylcholine (DOPC):

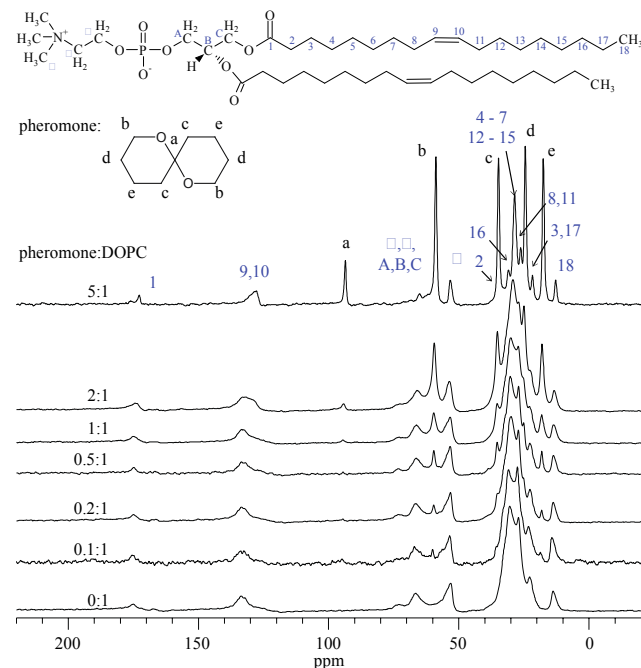


Figure 9. ¹³C spectra, recorded with high-power decoupling from ¹H nuclei, of 60% w/w DOPC/D₂O dispersion with different concentrations of pheromone (reported in figure as pheromone:DOPC mole ratios), with peak assignment.

The linewidth of the phospholipid chain signals is further reduced at high pheromone content (5:1 ratio), in agreement with the formation of the isotropic I_{II} phase, observed from ³¹P NMR spectra. We note that, due to the presence of the C=O carbonyl groups and of the C=C double bond, carbons 1, 9, and 10 (peaks at about 175 and 133 ppm) have a higher CSA, and show an inversion in the chemical shift tensor symmetry in passing from the 1:1 to the 2:1 ratio, in agreement with the L_α-H_{II} transition.

Another interesting feature is the isotropic chemical shift of the carbon of the terminal methyl group of DOPC chains, that resonates at 15.3 ppm in the DOPC/D₂O dispersion: by increasing the amount of uptaken pheromone the chemical shift regularly decreases down to 14.4 ppm in the sample with the 5:1 pheromone/DOPC mole ratio. The same effect was observed in the samples where deuterated cyclohexane replaced the pheromone (spectra not reported), suggesting that in both cases the uptaken molecules reside close to the terminal groups of the DOPC chains. This particular situation forces DOPC in the L_α phase to progressively remove the interdigitation of the two aliphatic layers. This result is in good

agreement with the SAXS data, that indicate an increment in the d spacing of the lamellar phase with increasing pheromone concentrations. This mechanism favours the transition to the H_{II} phase, where the uptaken molecules are moved to the hydrophobic cavities.

3.3.3. ^2H NMR

Static spectra. ^2H static spectra are very sensitive to the dynamic situation of deuterium nuclei and, in particular, to the rate and geometry of the motions involving the rigid fragment which the deuterium nucleus belongs to. In this study, ^2H spectra were recorded for the DOPC/ D_2O /pheromone and DOPC/ H_2O /cyclohexane- d_{12} mixtures with the twofold goal of obtaining dynamic information on the water and on the hydrophobic molecules.

The spectra recorded for the DOPC/ D_2O /pheromone samples are shown in Figure 10 (left).

The spectrum obtained in the absence of pheromone shows a quite "anomalous" lineshape: indeed, this is different from those previously reported in the literature for an L_α phase with a similar DOPC/ D_2O molar ratio (1:24),⁵⁸ arising from the superposition of an isotropic peak of extra-lamellar water and a Pake pattern due to inter-lamellar one. However, in contrast with these findings, Zhou - mainly through ^1H MAS spectra - found that all the water is inter-lamellar up to a DOPC/ H_2O ratio of 1:40.⁵⁹

Nonetheless, our spectrum could arise from the presence of water molecules in different situations, for instance more strongly or loosely bound to the phospholipid heads, substantially non-exchanging on the NMR time scale. The same effect on the NMR spectrum could also arise from a non-uniform distribution of inter-lamellar spacings. Another explanation is the presence of a slightly defective lamellar phase, in which some lamellae could have finite dimensions or some "holes", as observed in surfactant/water systems,^{60,61} or in which the bilayers could have a slight curvature, similarly to what observed in the "ripple" phase of phospholipid/water systems.⁶² In any case these effects could be due to the fact that the sample did not completely reach the "equilibrium" state.

All this considered, it must be noted that after adding a small amount of pheromone to the DOPC/ D_2O system a substantial change in the ^2H lineshape is observed. In particular it

becomes a Pake pattern, typical of inter-lamellar water molecules in the L_α phase, indicating that such phase reached a complete equilibrium. The narrow peak superimposed to the Pake pattern is very weak and must be ascribed to condensed water vapor from moisture in the sample tubes. Therefore, in any case, no extra-lamellar water is detected, in agreement with Zhou⁵⁹ and in disagreement with Volke.⁵⁸ The addition of further amounts of pheromone does not produce any relevant change in the ^2H lineshape up to the transition to the H_{II} phase occurs, as observed by ^{31}P . This causes an overall reduction of the linewidth and a progressive decrease of the Pake pattern associated with the L_α phase. This pattern is completely absent in the spectrum of the sample with the 5:1 ratio, which arises from the superposition of an anisotropic lineshape due to the H_{II} phase and an isotropic peak due to the I_{II} phase, in agreement with the ^{31}P results.

The spectra recorded for the set of samples DOPC/ H_2O /cyclohexane- d_{12} are reported in Figure 10 (right).

The lineshape obtained at the lowest concentrations arises from the partially anisotropic average of the quadrupolar interaction due to three different fast motions: rotation about the C_3 symmetry axis, tumbling of this axis respect to the local phase director (normal to the surface of the double layer), and chair-chair interconversion.⁶³ The experimental quadrupolar splitting corresponds to an order parameter of -0.037, which indicates that the C_3 symmetry axis tends to have a slight preferential orientation perpendicular to the double layers. The order parameter obtained is in agreement with those reported for the terminal ends of the phospholipid chains in the double layers,⁶⁴ confirming that the cyclohexane molecules are located near the methyl end groups of the hydrocarbon chains, as already inferred from the ^{13}C spectra. At higher cyclohexane concentrations an isotropic peak progressively rises, becoming the only peak when the cyclohexane:DOPC mole ratio is 5:1. This is in agreement with the location of cyclohexane molecules within the hydrophobic cavities in the H_{II} phase, where they no longer have a preferential orientation and can experience isotropic reorientational motions.

3.3.4. Spin-lattice relaxation times

Additional information on the dynamic behavior of water molecules, and in particular on motions with characteristic frequencies of the order of tens of MHz, could be obtained by measuring ^2H spin-lattice relaxation times (T_1)⁶⁵ in the DOPC/ D_2O /pheromone samples. The trend of ^2H T_1 vs. temperature for DOPC/ D_2O is reported in Figure 11a.

The relaxation time regularly increases with increasing temperature, clearly indicating that the motions contributing to the relaxation are in the fast motional regime (characteristic frequencies larger than ^2H Larmor frequency, here 61.4 MHz). Hence the decreasing trend detected for this relaxation time with increasing pheromone content (Figure 11b) reflects a decrease in the motional characteristic frequency. Therefore larger amounts of pheromone produce a reduction in the mobility of water molecules. This is in good agreement with the reduction of the inter-lamellar layers with increasing pheromone content observed by SAXS (see Table 4).

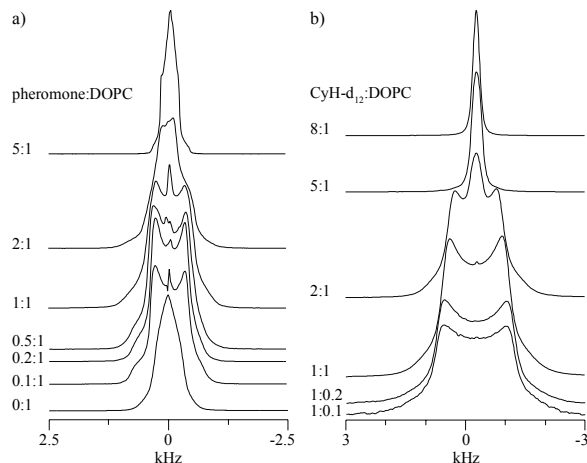


Figure 10. ^2H NMR spectra of: (left) 60% w/w DOPC/ D_2O dispersion with different concentrations of pheromone; (right) 60% w/w DOPC/ H_2O dispersion with different concentrations of cyclohexane- d_{12} .

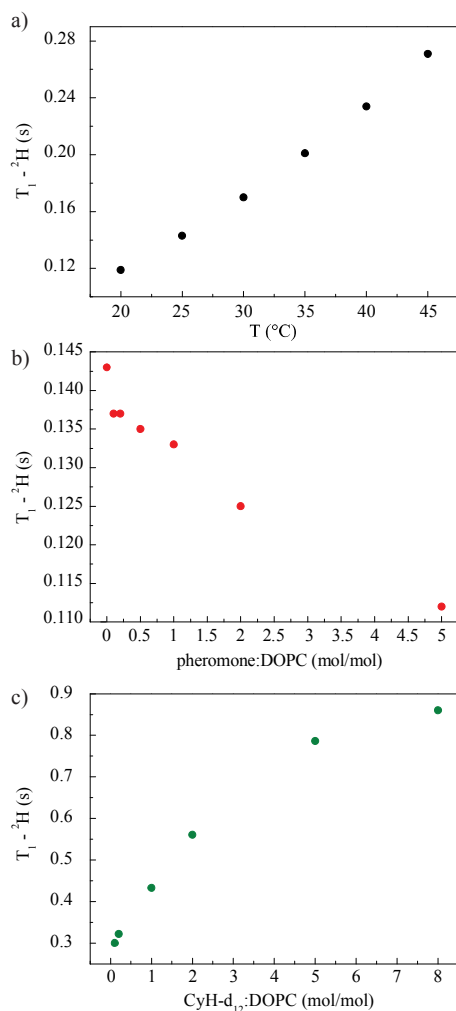


Figure 11. ^2H spin-lattice relaxation time T_1 of: (a) deuterated water in a 60% w/w DOPC/ D_2O dispersion, as a function of temperature; (b) deuterated water in a 60% w/w DOPC/ D_2O dispersion, at room temperature, as a function of the concentration of uptaken pheromone; (c) of cyclohexane- d_{12} (indicated as CyH- d_{12}) in 60% w/w DOPC/ H_2O dispersion, at room temperature, as a function of cyclohexane- d_{12} concentration.

On the other hand, the measurement of ^2H T_1 for the DOPC/ H_2O /Cyclohexane- d_{12} samples provides some information on the dynamics of the host molecule and of the aliphatic chains of the phospholipid. Figure 11c shows that the relaxation time increases with the amount of uptaken cyclohexane, indicating an increased characteristic frequency of the motion contributing to T_1 , that should correspond to an increased mobility of the aliphatic phospholipid chains, in agreement with the results obtained from the ^{13}C spectra.

4. Conclusions

The uptake of a very hydrophobic guest (1,7-dioxaspiro[5.5]undecane or “olean”) by a DOPC/water lamellar phase was investigated through SAXS, DSC and NMR. The results of this multidisciplinary investigation indicate that the addition of the hydrophobe has a significant impact on the phase structure of the lipid bilayer, bringing about a L_α - H_{II}

phase transition followed by a H_{II} - I_{H} phase change. NMR results confirm the hydrophobe in the phospholipid chains domains, and in particular in proximity to the terminal methyl groups. The phase changes induced by the uptake of the hydrophobe also a slowing down in the water reorientational motions and a lowering in its freezing temperature, both related to an increasing water confinement.

SAXS data confirm the structural changes detected by NMR experiments. DSC scans indicate that the L_α - L_α phase transition and the water melting change, depending on the uptake of olean into the DOPC/water nanostructure.

In conclusion, these results seem to confirm that the penetration of a strong hydrophobe (in this case a pheromone) in a biomimetic lipid bilayer (DOPC/water) has profound consequences on the packing of the lipid molecules in the self-assembly, and also on the distribution and properties of the hydration water molecules. Actually the packing change of the lipid and the properties of the aqueous pool seem to be two intertwined phenomena that mutually affect one another. More work is needed to deepen this important issue.

These findings point out that the interplay of phase changes and variation in the hydration of the lipid polar head groups can be - at least partly - involved in the mechanism that drive the nerve conduction process in all the natural and physiological cases in which it is at work.

Acknowledgements

The authors gratefully acknowledge CSGI for partial financial support and the Enzo Ferroni Foundation for helpful discussions.

References

- 1 B. W. Ninham and P. Lo Nostro, *Molecular Forces and Self Assembly. In Colloid, Nano Sciences and Biology*, Cambridge University Press, Cambridge, UK, 2010.
- 2 S. Turkyilmaz, P. F. Almeida and S. L. Regen, *Langmuir*, 2011, **27**, 14380.
- 3 R. Reigada, *J. Phys. Chem. B*, 2011, **115**, 2527.
- 4 Z. Yi, M. Nagao and D. P. Bossev, *J. Phys. Conf. Ser.*, 2010, **251**, 012037.
- 5 H. Tsuchiya, T. Ueno, M. Mizogami and K. Takakura, *Chem. Biol. Interact.*, 2010, **183**, 19.
- 6 T. T. Nguyen, J. L. Swift, M. C. Burger and D. T. Cramb, *J. Phys. Chem. B*, 2009, **113**, 10357.
- 7 D. Huang, T. Zhao, W. Xu, T. Yang and P. S. Cremer, *Anal. Chem.*, 2013, **85**, 10240.
- 8 K. Hichiri, O. Shirai and K. Kano, *Anal. Sci.*, 2012, **28**, 45.
- 9 N. P. Franks, *Nature Rev. Neurosci.* 2008, **9**, 370-386.
- 10 J. A. Campagna, K. W. Miller, D.Phil. and S. A. Forman, *N. Engl. J. Med.* 2003, **348**, 2110.
- 11 A. Kopp Lugli, C. S. Yost and C. H. Kindler, *Eur. J. Anaesthesiol.* 2009, **26**, 807.
- 12 E. N. Brown, R. Lydic and Nicholas D. Schiff, *N. Engl. J. Med.* 2010, **363**, 2638.
- 13 I. Ueda and T. Yoshida, *Chem. Phys. Lipids*, 1999, **101**, 65.
- 14 I. Ueda, H. S. Tseng, Y. Kaminoh, S.-M. Ma, H. Kamaya and S. H. Lin, *Mol. Pharm.*, 1986, **29**, 582.
- 15 I. Ueda, *Keio J. Med.*, 2001, **50**, 20.

- 16 M. Baciú, M. C. Holmes and M. S. Leaver, *J. Phys. Chem. B*, 2007, **111**, 909.
- 17 B. W. Urban, M. Bleckwenn and M. Barann, *Pharmacol. & Therap.*, 2006, **111**, 729.
- 18 R. Sogaard, T. M. Werge, C. Bertelsen, C. Lundbye, K. L. Madsen, C. H. Nielsen and J. A. Lundbaek, *Biochemistry*, 2006, **45**, 13118.
- 19 H. Tsuchiya, T. Ueno, M. Mizogami and K. Takakura, *Chem. Biol. Interact.*, 2010, **183**, 19.
- 20 X. Wang and Q.-X. Jiang, *J. Med. Mol. Biol.*, 2012, **9**, 425.
- 21 M. Weinrich and D. L. Worcester, *J. Phys. Chem. B*, 2013, **117**, 16141.
- 22 K. Larsson, *Langmuir*, 1988, **4**, 215.
- 23 C. Bandejas, A. P. Serro, K. Luzyanin, A. Fernandes and B. Saramago, *Eur. J. Pharm. Sci.*, 2013, **48**, 153.
- 24 M. Weinrich, H. Nanda, D. L. Worcester, C. F. Majkrzak, B. B. Maranville and S. M. Bezrukov, *Langmuir*, 2012, **28**, 4723.
- 25 H. Tsuchiya, T. Ueno, M. Mizogami and K. Takakura, *J. Anesth.*, 2010, **24**, 639.
- 26 M. Engelke, R. Jessel, A. Wiechmann and H. A. Diehl, *Biophys. Chem.*, 1997, **67**, 127.
- 27 D. Uhríková, G. Rapp, S. Yaradaikin, V. Gordeliy and P. Balgavý, *Biophys. Chem.*, 2004, **109**, 361.
- 28 S. Turkyilmaz, W.-H. Chen, H. Mitomo and S. L. Regen, *J. Am. Chem. Soc.*, 2009, **131**, 5068.
- 29 M. A. Knackstedt and B. W. Ninham, *Phys. Rev. E*, 1994, **50**, 2839.
- 30 K.-E. Kaissling, *Chem. Senses*, 1996, **21**, 257.
- 31 K. Mori, *Chem. Commun.*, 1997, 1153.
- 32 K. Takeda, Y. Sano, S. Ichikawa, Y. Hirata, H. Matsuki and S. Kaneshina, *J. Oleo Sci.*, 2009, **58**, 369.
- 33 L. Stowers and T.-H. Kuo, *Curr. Op. Neurobiol.*, 2015, **34**, 103.
- 34 J. Y. Yew and H. Chung, *Progr. Lipid Res.*, 2015, **59**, 88.
- 35 R. M. McKinney, C. Vernier and Y. Ben-Shahar, *Curr. Op. Insect Sci.*, 2015, **12**, 86.
- 36 C. A. Oi, J. S. van Zweden, R. C. Oliveira, A. van Oystaeyen, F. S. Nascimento and T. Wenseleers, *Bioessays*, 2015, **37**, 808.
- 37 J. Nardella, M. Terrado, N. S. Honson and E. Plettner, *Arch. Biochem. Biophys.*, 2015, **579**, 73.
- 38 A. Papachristoforou, A. Kagiava, C. Papaefthimiou, A. Termentzi, N. Fokialakis, A.-L. Skaltsounis, M. Watkins, G. Arnold and G. Theophilidis, *PLoS One*, 2012, **7**, e47432.
- 39 A. S. Ulrich, M. Sami and A. Watts, *Biochim. Biophys. Acta*, 1994, **1191**, 225.
- 40 D. G. Cory and W. M. Ritchey, *J. Magn. Reson.*, 1988, **80**, 128.
- 41 K. Eichele and R. E. Wasylshen, *WSOLIDS NMR Simulation Package*, 2000.
- 42 T. Blanton, T. C. Huang, H. Toraya, C. R. Hubbard, S. B. Robie, D. Louer, H. E. Gobel, G. Will, R. Gilles and T. Raftery, *Powder Diff.*, 1995, **10**, 91.
- 43 J. A. Lake, *Acta Cryst.*, 1967, **23**, 191.
- 44 R. P. Rand and N. L. Fuller, *Biophys. J.*, 1994, **66**, 2127.
- 45 S. C. Costigan, P. J. Booth and R. H. Templer, *Biochim. Biophys. Acta*, 2000, **1468**, 41.
- 46 S. Tristram-Nagle, H. I. Petrache and J. F. Nagle, *Biophys. J.*, 1998, **75**, 917.
- 47 M. Sjölund, G. Lindblom, L. Rilfors and G. Arvidson, *Biophys. J.*, 1987, **52**, 145.
- 48 R. N. A. H. Lewis, B. D. Sykes and R. N. McElhaney, *Biochemistry*, 1988, **27**, 880.
- 49 T. Heimburg and A. D. Jackson, *PNAS*, 2005, **102**, 9790.
- 50 E. Rowe *Mol. Pharm.*, 1982, **22**, 133.
- 51 R. Winter and C. Jeworrek, *Soft Matter*, 2009, **5**, 3157.
- 52 A. S. Ulrich and A. Watts, *Biophys. Chem.*, 1994, **49**, 39.
- 53 A. Nilsson, A. Holmgren, G. Lindblom, *Biochemistry*, 1991, **30**, 2126.
- 54 C. Dolle, P. Magrone, S. Riva, M. Ambrosi, E. Fratini, N. Peruzzi and P. Lo Nostro, *J. Phys. Chem. B*, 2011, **115**, 11638.
- 55 Z. Chen, L. C. M. Van Gorkom, R. M. Eppand and R. E. Stark, *Biophys. J.*, 1996, **70**, 1412.
- 56 C. P. S. Tilcock, P. R. Cullis and S. M. Gruner, *Chem. Phys. Lipids*, 1986, **40**, 47.
- 57 J. Mason, *Solid State Nucl. Magn. Reson.*, 1993, **2**, 285.
- 58 F. Volke, S. Eisenblatter, J. Galle and G. Klose, *Chem. Phys. Lipids*, 1994, **70**, 121.
- 59 Z. Zhou, B. G. Sayer, D. W. Hughes, R. E. Stark and R. M. Eppand, *Biophys. J.*, 1999, **76**, 387.
- 60 G. Chidichimo, N. A. P. Vaz, Z. Yaniv and J. W. Doane, *Phys. Rev. Lett.*, 1982, **49**, 1950.
- 61 P. L. Hubbard, K. M. McGrath and P. T. Callaghan, *J. Phys. Chem. B*, 2006, **110**, 20781.
- 62 L. M. Strenk, P. W. Westerman, N. A. P. Vaz and J. W. Doane, *Biophys. J.*, 1985, **48**, 355.
- 63 R. Poupko and Z. Luz, *J. Chem. Phys.*, 1981, **75**, 1675.
- 64 N. Boden, S. A. Jones and F. Sixl, *J. Am. Chem. Soc.*, 1991, **30**, 2146.
- 65 B. Cowan, *Nuclear Magnetic Resonance and Relaxation*, Cambridge University Press, Cambridge, UK, 1997.